First Supra-THz Heterodyne Array Receivers for Astronomy With the SOFIA Observatory

Christophe Risacher, Rolf Güsten, Jürgen Stutzki, Heinz-Wilhelm Hübers, Denis Büchel, Urs U. Graf, Stefan Heyminck, Cornelia E. Honingh, Karl Jacobs, Bernd Klein, Thomas Klein, Christian Leinz, Patrick Pütz, Nicolas Reyes, Oliver Ricken, Hans-Joachim Wunsch, Paul Fusco, and Stefan Rosner

***Abstract*—We present the upGREAT THz heterodyne arrays for far-infrared astronomy. The low-frequency array (LFA) is designed to cover the 1.9–2.5 THz range using 2 × 7-pixel waveguide-based HEB mixer arrays in a dual polarization configuration. The high-frequency array (HFA) will perform observations of the [OI] line at ∼4.745 THz using a 7-pixel waveguide- based HEB mixer array. This paper describes the common design for both arrays, cooled to 4.5 K using closed-cycle pulse tube technology. We then show the laboratory and telescope characterization of the first array with its 14 pixels (LFA), which culminated in the successful commissioning in May 2015 aboard the SOFIA airborne observatory observing the [CII] fine structure transition at 1.9005 THz. This is the first successful demonstration of astronomical observations with a heterodyne focal plane array above 1 THz and is also the first time high-power closed-cycle coolers for temperatures below 4.5 K are operated on an airborne platform.**

***Index Terms*—Cryogenics, far-infrared astronomy, HEB mixer, heterodyne, receivers, submillimeter-wave technology, superconducting devices.**

I. Introduction

With the successful Herschel observatory satellite mission, which was active between 2009–2012 [1], astronomical observations over the 1–5-THz range were performed with order of magnitude of improved sensitivities, compared with previous satellite missions. This far-infrared region cannot be explored from ground-based telescopes (with the exception of narrow frequency windows observable from high-altitude locations). The instrumentation for this wavelength range is divided into two types: direct detection cameras, which can have low- to mid-resolution spectroscopic capabilities, and heterodyne receivers, which provide very high-resolution spectroscopy. The main reason for wanting high resolution is to resolve the spectral lines profiles, which allows studying the gas excitation and kinematics in great detail.

The continuum-type instrumentation routinely incorporates several hundred or more pixels, and there is rapid progress in this area [2]–[4]. For high-resolution spectroscopy using heterodyne receivers, only recently did the detector sensitivities start approaching their fundamental noise limit up to very high frequencies [5], [6], and the next step is now to increase the receiver pixels count in order to gain observing efficiency when observing extended sources. The review papers [7], [8] summarize the current status of multi-pixel heterodyne array receivers for the sub-mm, far-infrared region and present general design considerations. Until now, only small sized arrays have been realized in a handful of observatories for frequencies between 0.3–0.8 THz (e.g., [9]–[12]) and only single pixel receivers have been successfully operated on telescopes for frequencies above 1 THz (e.g., [13]–[15]). Several THz array projects are ongoing and concepts have been presented for THz heterodyne arrays (e.g., [16]–[18]) but, until now, none has been successfully operated on a telescope. Several satellite missions for the far-infrared region (SPICA [19], Millimetron [20]) and balloon experiments (STO-2 as successor of STO [13] or GUSTO) plan to use array instruments in the future. Currently, the SOFIA[1] airborne observatory, a NASA/DLR operated Boeing 747 carrying a 2.5-m telescope, is the only platform capable of observing in that wavelength region [21].

Among the SOFIA instruments, the only one able to achieve high resolution spectroscopy (above 10^6 resolving power) is the GREAT instrument [22]. In this paper, we present the new array receivers for this instrument, the upGREAT multi-pixel heterodyne arrays for frequencies 1.9–2.5 THz and 4.75 THz.

Manuscript received September 01, 2015; revised November 03, 2015, December 08, 2015; accepted December 08, 2015. Date of publication December 28, 2015; date of current version March 21, 2016 This work was supported in part by the Federal Ministry of Economics and Technology via the German Space Agency (DLR)under Grant 50 OK 1102, Grant 50 OK 1103, and Grant 50 OK 1104 and by the Collaborative Research Council 956, sub-projects D3 and S, funded by the Deutsche Forschungsgemeinschaft (DFG).

C. Risacher, R. Güsten, S. Heyminck, and O. Ricken are with the Max Planck Institut für Radioastronomie, Bonn 53121, Germany (e- mail: crisache@mpifr.de).

J. Stutzki, C. Honingh, D. Büchel, U. U. Graf, K. Jacobs, and P. Pütz are with Cologne University, Köln 50937, Germany (e-mail: stutzki@ph1.uni-koeln.de).

H.-W. Hübers is with the German Aerospace Center (DLR), Institute of Optical Sensor Systems, Berlin 12489, Germany (e-mail: Heinz-Wilhelm.Huebers@dlr.de).

B. Klein is with the Max Planck Institut für Radioastronomie, Bonn 53121, Germany, and also with the University of Applied Sciences Bonn-Rhein-Sieg, Sankt Augustin 53757, Germany (e-mail: bklein@mpifr.de).

T. Klein is with the Max Planck Institut für Radioastronomie, Bonn 53121, Germany, and also with the European Southern Observatories, Vitacura, Santiago de Chile 19001, Chile (e-mail: tklein@eso.org).

N. Reyes was with the Max Planck Institut für Radioastronomie, Bonn 53121, Germany. He is now with the Universidad de Chile, Santiago, Chile (e-mail: nireyes@u.uchile.cl).

P. Fusco is with NASA Ames Research Center, Moffett Field, CA 94035 USA (e-mail: paul.r.fusco@nasa.gov).

S. Rosner is with the SETI Institute, Mountain View, CA 94043 USA (e- mail: stefan.rosner@nasa.gov).

Color versions of one or more of the figures in this paper are available online at http://ieeexplore.ieee.org.

Digital Object Identifier 10.1109/TTHZ.2015.2508005

[1]SOFIA is a joint project of NASA and the German Aerospace Center (DLR). The aircraft is based at the NASA Armstrong Flight Research Center (AFRC) facility in Palmdale, California which also manages the program. NASA Ames Research Center at Moffett Field, CA, USA, manages the SOFIA science and mission operations in cooperation with the Universities Space Research Association (USRA) headquartered in Columbia, MD, USA, and the German SOFIA Institute (DSI) at the University of Stuttgart.

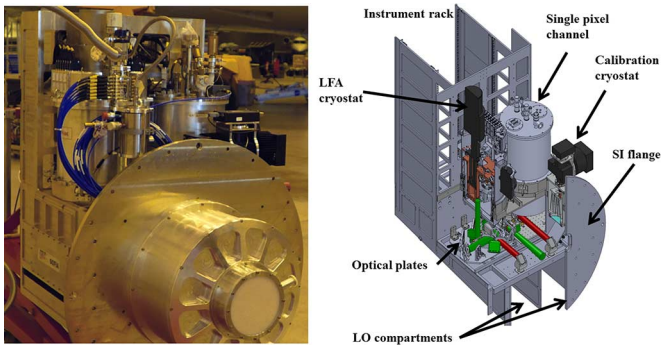

Fig. 1. In this example, the GREAT instrument accommodates the upGREAT LFA channel (left cryostat) and a single pixel cryostat (L1 band) operated simultaneously. A smaller cryostat contains the 80 K load used for calibration. The SI flange attaches to the telescope Nasmyth tube. The sky signal (in green) is separated either in polarization by a wire grid or in frequency by a dichroic filter. The local oscillator components are placed under the structure. The LO signals (in red) are coupled with the sky signal on an optical plate located inside the structure. Sensitive electronic components are located in the electronics rack section.

TABLE I
GREAT RECEIVER PERFORMANCE AS OF 2011 AND 2015

Bands	Characteristics	Performance May 2011	Performance January 2015
L1	Frequency range	1.25-1.5 THz	1.25-1.50 THz
	IF Bandwidth	1.0-2.5 GHz	0.2-2.5 GHz
	Trec (DSB)	1000 K-1750 K	500 K@0.5GHz
	LO coupling	Diplexer optics	Beam splitter optics
L2	Frequency range	1.81-1.91 THz	1.81-1.91 THz
	IF Bandwidth	1.0-2.5 GHz	0.2-2.5 GHz
	Trec (DSB)	1500 – 4000 K	600 K@0.5GHz
	LO coupling	Diplexer optics	Beam splitter optics
Ma	Frequency range	2.49-2.52 THz	2.49-2.52 THz
	IF Bandwidth	1.0-2.5 GHz	1.0-2.5 GHz
	Trec (DSB)	3000 K	1500 K@2GHz
	LO coupling	Diplexer optics	Diplexer optics
H	Frequency range		4.745 ± 0.004 THz
	IF Bandwidth		0.2-2.5 GHz
	Trec (DSB)		800 K@0.5GHz
	LO Technology		QCL
	LO coupling		Beam splitter optics

II. GREAT/upGREAT RECEIVERS

The GREAT instrument[2] is described in detail in [22]. Its modular construction allows using at any time two cryostats mounted on the main support structure, which is then mounted to the telescope Nasmyth flange (Fig. 1). Both cryostat channels observe in parallel the same sky position.

The main advantage of operating an airborne observatory as opposed to a satellite is the flexibility in placing newer developed technologies with very short turn-around times. Table I lists the available receiver bands and performance when GREAT was first installed in 2011 and after several years of operation, in January 2015. These are all single-pixel cryostats cooled with liquid nitrogen and liquid helium. A significant improvement can be seen in the receiver performance in Table I and is explained by various upgrades: 1) improved optics; 2) better hot electron bolometer (HEB) detectors; and 3) higher output power local oscillator solid state chains. Most noticeably, a new receiver band based on waveguide HEB mixers was added in 2014 [23], opening the [OI] 4.7-THz band for high-resolution spectroscopy for the first time since the pioneering Kuiper Airborne Observatory (KAO) in 1988–1995 [24].

[2]GREAT is a development by the MPI für Radioastronomie (Principal Investigator: R. Güsten) and the KOSMA/Universität zu Köln, in cooperation with the MPI für Sonnensystemforschung and the DLR Institut

TABLE II
upGREAT SPECIFICATIONS

	LFA array	HFA array
RF Bandwidth	1.9-2.5 THz	4.745 ± 0.004 THz
IF Bandwidth	0.2-4 GHz	0.2-4 GHz
HEB technology	Waveguide feedhorn antenna coupling, NbN HEB on Si membrane	Waveguide feedhorn antenna coupling, NbN HEB on Si membrane
LO technology	Photonic mixers / solid-state chains	Quantum cascade lasers (QCL)
LO coupling	Beamsplitter (goal) or Diplexer (baseline)	Beamsplitter
Array layout	2x7 pixels dual polar. in hexagonal layout with a central pixel	7 pixels single polar. in hexagonal layout with a central pixel
T_{REC}	Goal <1000K DSB	Goal <1500K DSB
Backends	0-4 GHz with min. 32k channels	0-4GHz with min. 32k channels

The new upGREAT receivers' main characteristics are listed in Table II. The low-frequency array (LFA) covers the 1.9–2.5-THz range using 2 × 7-pixel array (dual polarization). The high-frequency array (HFA) observes at 4.745 THz with a single polarization 7-pixel array. Each receiver channel is integrated in a single closed-cycle cryostat.

This paper presents the main design, testing, and verification for common parts of the LFA/HFA receivers and presents the LFA receiver final integration, laboratory characterization and subsequent commissioning campaign results. The cryocooler infrastructure aboard the Boeing 747 is also presented here.

III. upGREAT INSTRUMENT DESIGN

A. General Description

The main components of upGREAT are illustrated in Figs. 1 and 2. As for any heterodyne receiver system, a high-precision reference signal called local oscillator (LO) is required. The LO and the sky signal from the telescope are combined on an optics plate and are coupled to the superconducting HEB mixers. The intermediate frequency (IF) signal is amplified by cryogenic microwave low-noise amplifiers (LNAs) placed directly at the mixers output. The mixers and LNAs are located inside the cryostat and cooled to temperatures below 4.5 K. The IF signals are brought to the cryostat output connectors by stainless steel coaxial lines and are further amplified by room temperature amplifiers. The IF processor provides additional gain, equalization, filtering and computer-controlled output leveling of the IF signal, to match the nominal input level of the digital spectrometers.

In our case, the most demanding configuration is when the LFA and HFA arrays are used in parallel. In that case, up to 21 HEB mixers, cryogenic LNAs, warm amplifiers and IF signal chains are active (shown in Fig. 2). Until May 2015, at most two channels were used on the GREAT instrument, therefore,

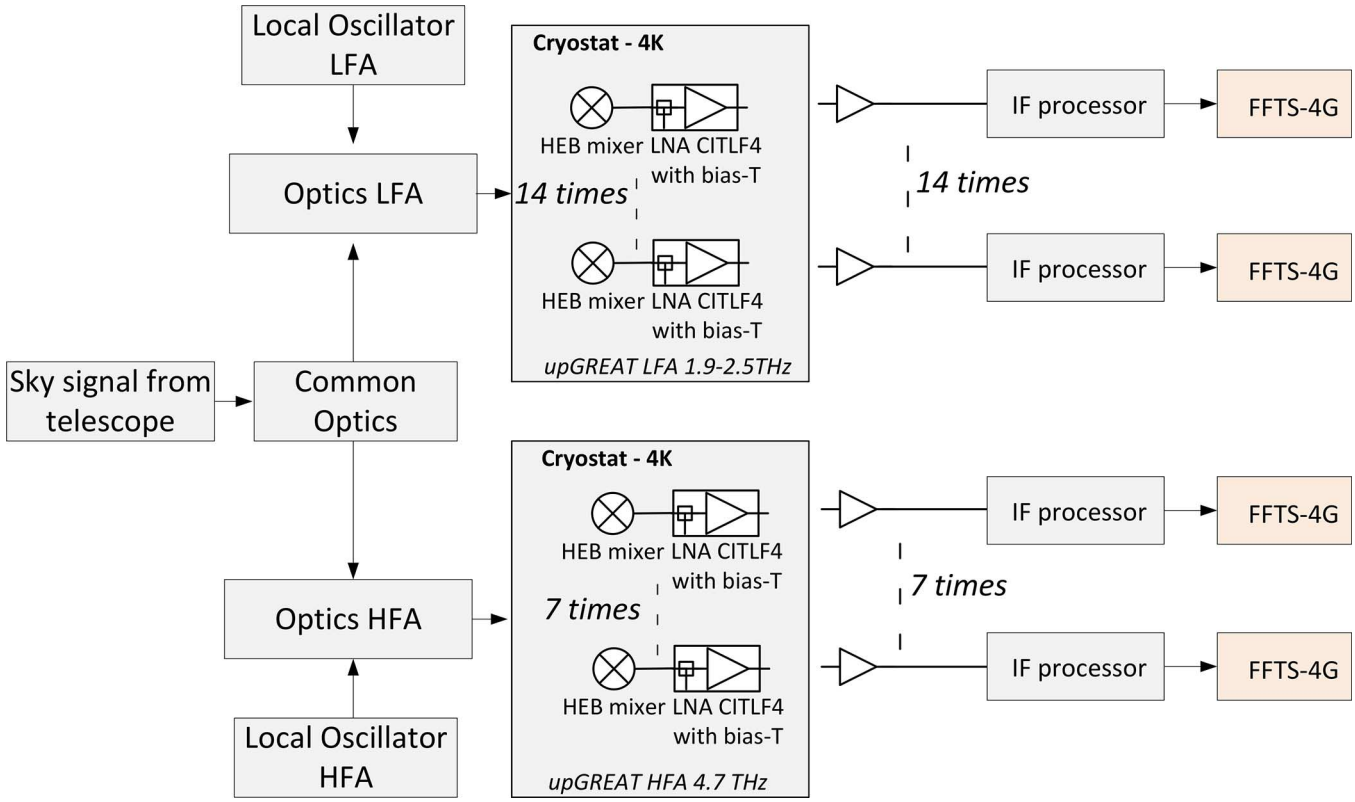

Fig. 2. General layout of the LFA/HFA configuration, when 14 + 7 signal chains are then needed.

all of the bias electronics, IF processor, and spectrometers were redesigned and upgraded to accommodate a maximum of 21 channels.

B. upGREAT LFA Local Oscillator

1) Introduction: The upGREAT LFA has a broad RF range going from 1.9 to 2.5 THz, and all of the components are designed to cover that range. The limiting factor at the moment is the availability of suitable LO sources with sufficient output power and RF bandwidth.

Solid-state multiplying chains are the current sources of choice, providing several tens of μW at 1.9 THz and with relative bandwidths of $\sim$10%. The other candidate as a source is the quantum cascade laser (QCL) which can produce several hundreds of μW power [25], [26]. In parallel, we are developing in-house at the MPIfR photonic mixer local oscillators to cover the full RF range, from 1.9 to 2.5 THz. Photomixer-based sources have demonstrated several μW of power at 1 THz [27]. Despite this promising result, this is not yet sufficient to pump our HEB detectors with a straightforward and broadband beam-splitter coupling optics. Once the photonic LOs demonstrate sufficient LO power (a minimum of a factor of 2 increase is needed), they will be used with the LFA receiver in subsequent flight series (one photo-mixer per HEB mixer). The modularity of the system allows an easy replacement of the existing LO module with future improved units.

2) General Description: For the first observing campaigns with the SOFIA observatory, the LO sources are solid state multiplying chains, developed by Virginia Diodes, Inc. [28]. Their main characteristics are presented in Table III. The frequency coverage is limited to 1.88 to 1.92 THz, centered to cover the [CII] transition. Those LO chains use novel technologies, such as diamond substrates for thermal management, in-phase combining networks, and power amplification at 30 GHz to achieve an output power of 20 μW at ambient temperature. To further increase the output power, the last two passive triplers are cooled to 80 K, effectively doubling the output power to about 40 μW.

TABLE III
UPGREAT LFA LO OPTICAL PARAMETERS

LO Bandwidth	1.882-1.920 THz (limited by the LO output power)
Output power	20 μW at ambient temperature 40 μW when last triplers are cooled to 80K
Optical coupling	Fourier Phase grating separates output beam into 7 equal amplitude beams

In order to provide sufficient LO power for both LFA subarrays (2 × 7 HEB mixers), two identical LO chains are used, one per polarization. The outputs for both chains have orthogonal polarizations and are combined via a wire grid located inside the LO cooler (Fig. 3 and 5). The resulting output LO beam is then split into seven equal beams by using a Fourier phase grating [29] designed to operate at a center frequency of 1.9 THz with about 10% usable bandwidth. Every output beam contains about 12.8% of the incident power (90% efficiency).

All of the LO adjustment optics and phase grating are therefore common to the combined LO signals. They are separated afterwards by another wire grid, located on the optical plate and couple afterwards to their respective LFA subarrays.

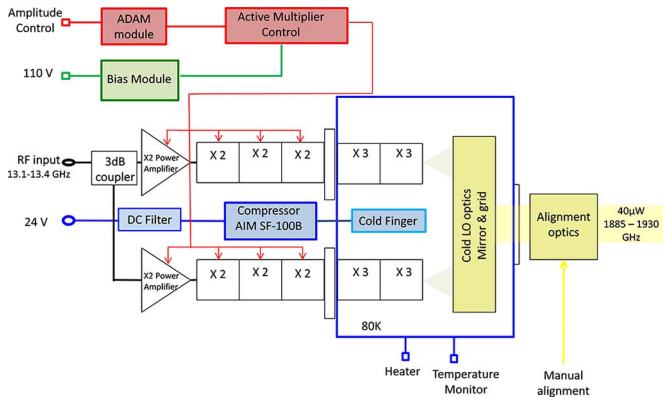

Fig. 3. LFA local oscillator general diagram. The identical chains AMC-410 and AMC-461 produce about 20 μW power at 1.9 THz and 40 μW when the last two triplers are cooled down to 80 K. The LO outputs are combined via a wire grid inside the LO cryostat.

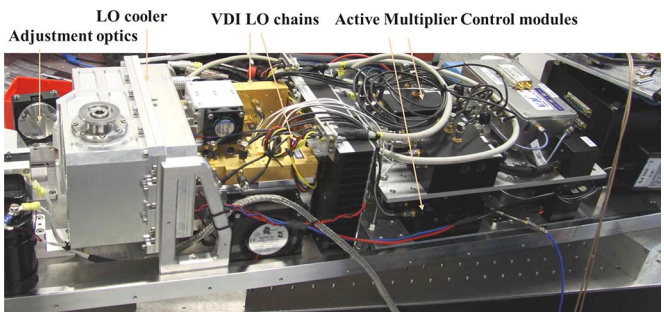

Fig. 4. LFA LO box assembly. The LO cryostat and warm adjustable optics are shown on the left-hand side. The active multiplier control modules provide the required bias to the various multipliers. The last two triplers of each chain, placed in the LO cryostat, are self-biased.

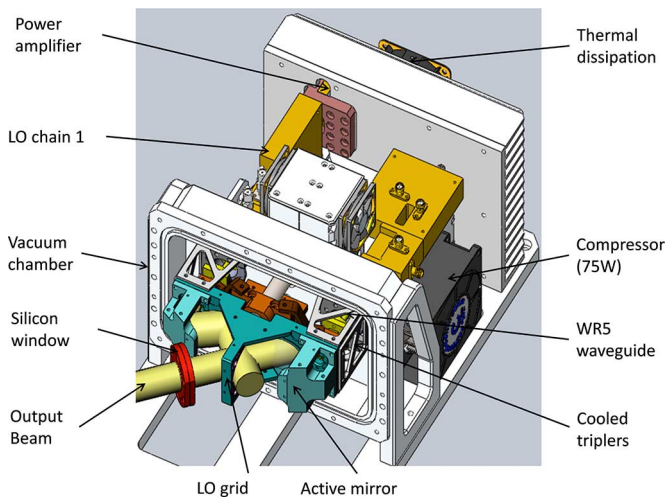

Fig. 5. View of the VDI LO chains together with the LO cooler (one half cover is removed). The combined LO output signal can be seen. The two LO chains are placed with 90 degrees polarization difference and the LO grid combines them at its output. The RF window is a 1-mm-thick Silicon with Parylene-C coating.

3) LO Cooler Design: The two solid-state chains are integrated with the control electronics power supplies and closed-cycle cooling machine in a compact module (Figs. 4 and 5). We use the AIM SF100 cooler, which is a Stirling cryocooler based on a moving magnet. It provides 2 W of cooling power at 80 K, consuming 75 W of electrical power. The last two triplers of each VDI LO chains are placed inside a small cryostat. The cold tip from the cooler is thermally connected to the triplers via flexible copper straps. To thermally isolate the triplers from the room temperature components, but keeping low insertion losses, 1″ stainless steel WR-5 waveguide pieces are placed between the last room temperature doubler and the first cooled tripler. The measured loss of such a waveguide is about 1.5 dB at 230 GHz. To further decrease these losses, the National Radio Astronomy Observatory (NRAO), Charlottesville, VA, USA, copper plated those waveguides. After plating with more than 10 μm thick copper, the losses at 230 GHz for the 1-in-long waveguides decreased to $\sim$0.5 dB.

The small LO cryostat optical window is a 1-mm-thick high-resistivity Silicon window from Tydex, LLC, coated on both sides with Parylene. The window is optimized for best transmission at 1.9 THz (above 88%).

4) Reference Synthesizer: The solid state multiplier chains need a +10 dBm reference signal in the 13.1–13.4-GHz range (multiplication factor is 144). The characteristics of the reference signal are critical, as the final phase and AM noises of the system strongly depends on it. Various types of high-performance lab bench synthesizers were successfully used to drive VDI multiplier chains for the GREAT single pixel receivers. However, for the upGREAT development, due to space and weight limitations on the instrument mounting structure, a more compact solution was needed. Several synthesizer modules were tested (VCO-based and YIG-based) covering 8–20 GHz. When comparing the overall receiver performance, the best results are achieved with the VDI synthesizer. The receiver sensitivity compares then very favorably to the lab-bench synthesizers (equal or better performance). Using other models, such as VCO-based synthesizers, the receiver noise temperature can degrade by up to 20%. We therefore selected the VDI synthesizers to drive the GREAT/upGREAT receivers.

C. HFA Array LO

The local oscillator source for the HFA receiver at 4.7 THz will be a QCL LO. A prototype has already been demonstrated [30], having more than 100-μW output power, intrinsic linewidths below 10 MHz, and is routinely used with the GREAT H-channel receiver. A parallel development is ongoing between the groups KOSMA at the Universität zu Köln and the DLR-Pf Berlin, for the final upGREAT HFA local oscillator.

D. Frontend Cryostat and Closed-Cycle Cooler

The cryostats accommodating the upGREAT mixer arrays are partly based on the GREAT cryostats design. Both have the same mechanical interface to fit the mechanical structure which connects to the telescope flange (see Fig. 1). Therefore, the external dimensions and mass for the upGREAT cryostats are severely constrained and must stay within fixed mechanical limits. CryoVac GmbH fabricated the upGREAT cryostats using the same process specifications as for the GREAT cryostats, which had already been certified for airworthiness.

The major difference between the GREAT single pixel receivers and the upGREAT multi-pixel receivers is the cooling

mechanism. The first generation of cryostats uses liquid nitrogen and liquid helium for cooling. However, with seven or 14 detectors, the cryostat space is limited, and power dissipation in the active components (LNAs) becomes too large in order to keep hold times above 15 h at 4.2 K (which is the minimum required onboard SOFIA for a full night of observations). This would require having much larger liquid N_2 and He tanks and then space and weight limitations become prohibitive to accommodate the arrays. It was therefore decided to use closed-cycle pulse tube coolers.

1) Pulse Tube Cooler: The receivers are cooled by closed-cycle pulse tube refrigerators, model PTD-406C from TransMIT GmbH [31]. The pulse tube was custom modified to accommodate a small 0.2 L helium pot, connected directly to the 2nd stage. It uses a separate helium circuitry, which allows liquefying He [32]. The minimum quantity of liquid helium to suppress almost completely the temperature fluctuations of the pulse tube was found to be 30 cm^3. The dampening is about a factor of 25, reducing peak-to-peak modulation of 300 mK, to less than 12 mK at the cold head.

One of the main selection criteria for the cooler was its ability to withstand large tilts with minor impact on the cooling performance. This model PTD-406C has very long tubes, which are less sensitive to convection losses. The specification was to be able to tilt the cooler to $\pm 45^\circ$ orthogonal to the telescope elevation axis with minor cooling degradation.

The pulse tube cooler provides about 0.8 W of cooling power at 4.2 K when using the Sumitomo air-cooled compressor CSA-71A which is the selected compressor to operate the LFA 14-pixel receiver. With the smaller Sumitomo air-cooled compressor (CNA-31C), the cooling power at 4.2 K is about 0.5 W, which is sufficient for use with the HFA 7-pixel array.

2) upGREAT Cryostats Design: The cryostats' main components are shown in Fig. 6. There are two cooling stages, at $\sim$40 K and $\sim$3 K. The pulse tube is connected to its rotary valve separated by a 0.75-m flexible helium line. This allows decoupling the rotary valve mechanical vibrations from the detectors if desired. In our case, the rotary valve is rigidly attached to the cryostats.

The pulse tube cooling stages are thermally connected to the first and second stage plates through flexible copper straps. Fiber glass structures provide the mechanical support for these stages and their components. They consist of two mounting flanges or rings with a G10 cylindrical structure in between them.

The outer vacuum walls of the upGREAT cryostats are separated into two parts, the lower one incorporating the vacuum RF windows. The windows are made of high resistivity 525-μ m-thick Silicon with etched linear grooves on both sides to act as matching layers at the wavelength of interest. They have above 90% transmission in the 1.9–2.5 THz range and 4.7-THz range [33]. For the LFA cryostat, the infrared filters used are one layer of Zitex G104, cooled to 40 K. For the HFA cryostat, the infrared filter is a QMC dichroic low-pass filter with an 8-THz cutoff frequency.

For the electrical wiring inside the cryostats, Lakeshore Phosphor-Bronze AWG-32 and AWG-36 dual-twist and quad-twist wires are used. To provide filtering, several sub-D and micro-D capacitive filter networks connectors are used, placed on the

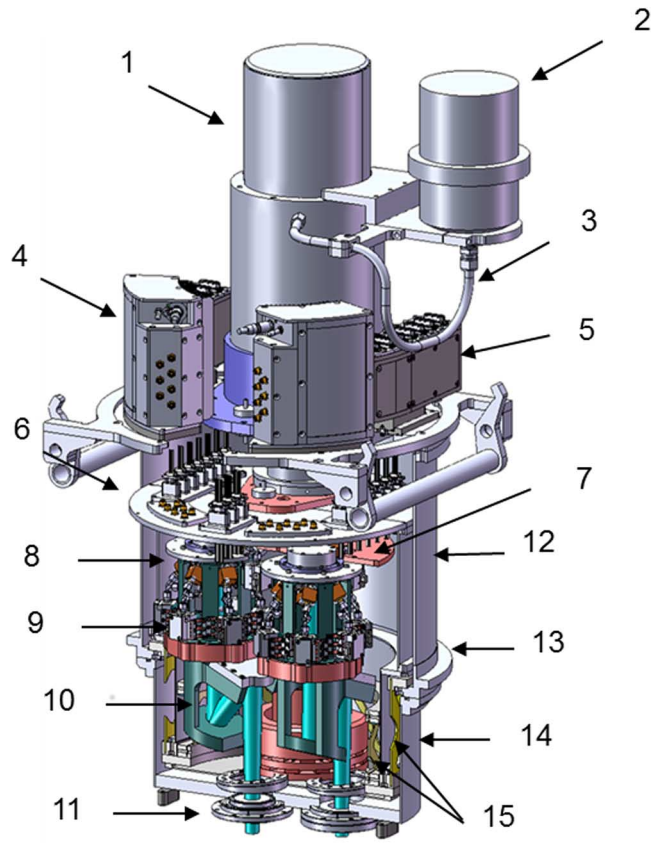

Fig. 6. upGREAT cryostat main components. (1) Pulse tube PTD-406C cold head. (2) Rotary valve. (3) Flexible Helium line. (4) Warm IF amplifiers. (5) Pre-amplifiers for biasing HEBs. (6) 40 K stage plate. (7) 4 K stage plate. (8) HEB detectors. (9) Cryogenic SiGe amplifiers. (10) Cold optics. (11) RF windows. (12) Vacuum vessel upper part. (13) Seal ring. (14) Vacuum vessel lower part. (15) Fiber glass Supports 4 K–40 K.

300 K and 40 K interfaces. The top plate accommodates the electrical feedthroughs (bias connectors, temperature and heater connectors and the coaxial SMA IF connectors). Pre-amplifier bias modules and warm IF amplifiers are directly mounted on this top plate (items 4–5 in Fig. 6).

3) Cryostats Cooling Performance: The summary of the cooling performance for the cryostats using various compressors is presented in Table IV.

For the 14-pixel LFA cryostat, the minimum base plate temperature is 2.5 K when the LNAs are turned off and increases to 2.8 K when they are nominally biased. The temperature on the detectors is about 4.2 K when using the CSA-71A compressor with 14 pixels, and 4.4 K when using the CNA-71A compressor with seven pixels. The tilting impact was verified by rotating the whole assembly including the cryostat by $\pm 45^\circ$. This confirmed that the second stage temperature stays stable within 1 mK and the first stage temperature within $<$200 mK.

The temperature fluctuations measured directly on the second stage plate were confirmed to be drastically minimized when liquefying Helium in the Helium pot. However, the measured temperature fluctuations on the mixer blocks were sufficiently small (below 1 mK peak to peak) so that using the external Helium circuitry for liquefaction was not necessary in the final flight configuration.

TABLE IV
UPGREAT COOLING PERFORMANCE

Compressor	CNA-31C	CSA-71A
Compressor input power	~3.5 kW	~8.0 kW
Cooling Power 1st stage	10 W @60 K	10 W @45 K
Cooling Power 2nd stage	0.5 W @4.2 K	0.8 W @4.2 K
Cold end temperature	3.0 K	2.8 K
Mixer physical temperatures on blocks	4.4 K average with 7 pixels (HFA band)	4.2 K average with 14 pixels (LFA band)
Temperature Fluctuations	±150 mK on base plate ±6 mK with >30 cm^3 LHe in Helium pot	±150 mK on base plate ±6 mK with >30 cm^3 LHe in Helium pot
Cooling time	24 h to 3.5 K 60 h to 3.0 K	17 h to 3.3 K 60 h to 2.8 K
Tilt impact (±45°)	< 200 mK change on 1st stage < 1 mK change on 2nd stage	< 200 mK change on 1st stage < 1 mK change on end stage

TABLE V
SOFIA—OPTICAL PARAMETERS

Primary diameter	2500 mm
Primary focal length	3200 mm
Telescope focal length	4914 mm
Blockage	522 mm

TABLE VI
UPGREAT—DESIGNED OPTICAL PARAMETERS

	LFA	HFA
RF Bandwidth	1.9-2.5 THz	4.7 THz ± 4 GHz
Edge Taper	13 dB	13 dB
Beam waist at SOFIA focal plane	2.4 mm at 1.9 THz 1.7 mm at 2.5 THz	1.0 mm
Half Power Beam Width (HPBW)	15.5" at 1.9 THz 11.8" at 2.5 THz	6.3"
Pixel spacing on sky	34.0"	13.8"

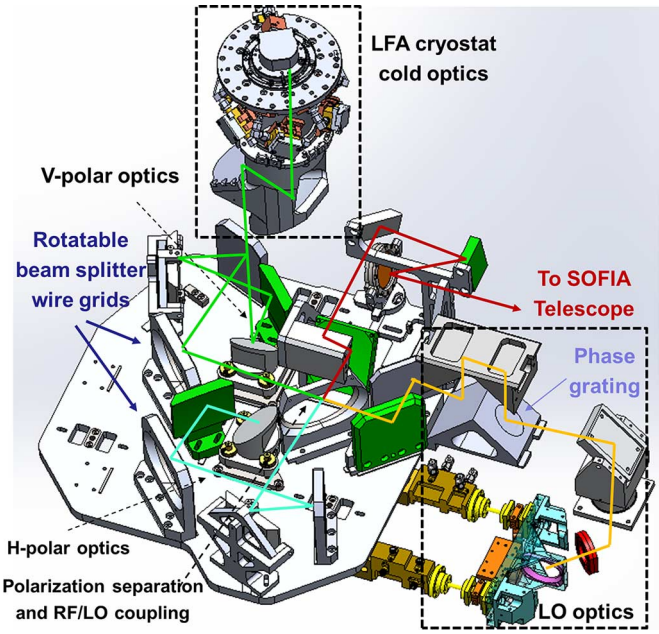

Fig. 7. View of a main optical components. The LO beam path from the two VDI chains is shown in orange, the input RF signal from SOFIA is shown in red. The combined RF/LO signals for both polarizations are shown in green and light blue. The active mirrors are drawn in green.

E. Optics Design

1) Common Optics: The main SOFIA telescope optical characteristics are summarized in Table V. Details of the telescope common optics can be found in [21]. The SOFIA telescope nominal waist position is located 300 mm away from the SI flange interface, towards the instrument. With the upGREAT arrays, a mirror-type derotator is used to compensate for the sky rotation in the focal plane of the telescope, which happens on this type of Alt-Az mount telescopes. It consists of three optical quality flat mirrors mounted on a rotational stage. The derotator is computer controlled and can compensate for the sky rotation. With this, the pixel pattern can be kept fixed on sky (in the equatorial or instrument reference systems) or rotated as desired, allowing for different, sophisticated observing strategies.

2) LFA Coupling Optics: The main designed optical parameters of the LFA array are summarized in Table VI. The telescope secondary edge taper was chosen to be 13 dB. The pixel spacing is then 2.2 × HPBW at 1.9 THz corresponding to 34 arcseconds on sky. The beam spacing at the mixer focal plane position is 12 mm, and the beam spacing at the SOFIA focal plane position is 8 mm, therefore the magnification factor was designed to be 1.5. The optical design consists of a pair of Gaussian telescopes, of magnifications 1.35 and 1.1. The optical design is solely based on reflective optics (no lenses are used). The main components are shown in Fig. 7.

The first LFA optical design (Fig. 8) is based on diplexers to allow using local oscillators with limited output power, which is the case for frequencies above 1.9 THz, where LO sources are scarce and limited. A description of this type of optical design for array receivers using a pair of Gaussian telescope and diplexers can be found in [8], [12].

A second optical plate was manufactured identical to the first design replacing the diplexers with beam splitter wire grids and including additional mirrors to keep the same overall path length. This is of interest when there is sufficient LO power available. The wire grids can be manually rotated to vary the LO coupling from 15% to 40% while also allowing the usage of the full IF bandwidth of the HEB mixers.

The main advantage of a diplexer-based LO coupling optics is that all of the LO power is effectively used. The limitations are that it is very difficult to achieve identical path-lengths for all offset pixels, causing sensitivity degradation [34], the IF bandwidth is limited to at best 1.5 GHz (having the most sensitive lower IF blocked by the diplexer) and the added complexity of diplexers often cause receiver instabilities. Therefore, depending on the amount of LO power available, either the diplexer or beam-splitter coupling optics can be used.

3) HFA Coupling Optics: The HFA optics design is a scaled version of the LFA beam splitter coupling optics. The optical design of the HFA is summarized in Table VI (last column). The spacing between the pixels is 2.2 × HPBW at 4.7 THz (edge taper of 13 dB). The beam spacing at the mixer locations is 10.5 mm, and the beam spacing at the SOFIA focal plane position is 3.5 mm, therefore the magnification factor is designed

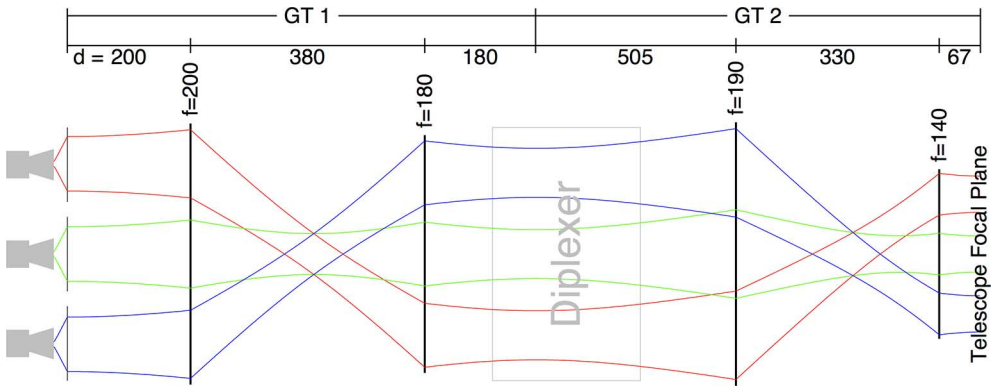

Fig. 8. Schematic beam path using two Gaussian telescopes for reimaging. The LO diplexer can be placed if needed between them. The cryostat window is located at an image of the telescope aperture, where the total beam cross section is minimal. For compactness and clarity, imaging elements are drawn as lenses, although mirrors are more commonly used in real instruments.

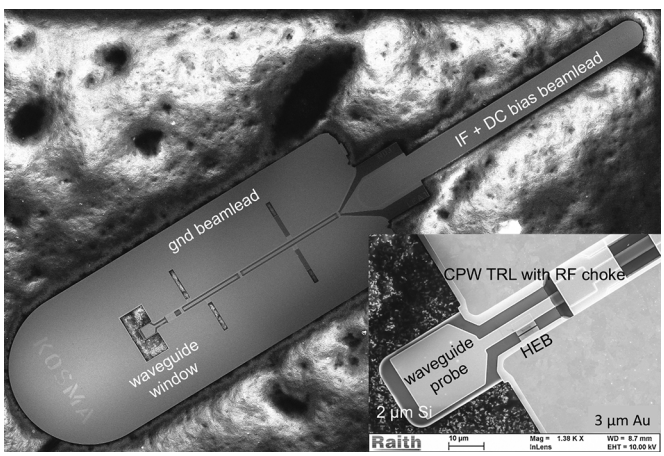

Fig. 9. View of a HEB NbN device for the LFA array. The ground contacts are done via the large beamleads. The IF output beamlead is bonded to a transmission line on a separate circuit board and for strain relief this TRL is wire bonded to the center conductor of a SMA connector.

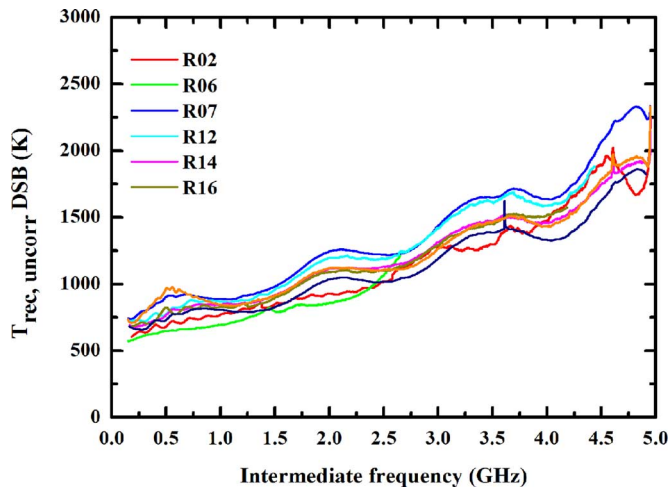

Fig. 10. Noise-temperature characterization of the LFA mixers in a test cryostat. No corrections were applied with approximately 90% signal coupling and non-evacuated signal path. The devices are from one section "R" of the flight devices wafer and the mixers are used in the H polarization array.

to be 3.0. The optical design consists of a pair of Gaussian telescopes, each of magnification 1.5 and 2.0.

F. HEB Mixers

The superconducting detectors are Hot Electron Bolometers developed by the KOSMA group at the Universität zu Köln, with state of the art performance. The NbN HEB mixers fabrication used for upGREAT is described in [23], [35].

1) LFA HEB Mixers: The HEB mixers designed for the LFA receiver cover the complete RF bandwidth from 1.9 to 2.5 THz using a broadband single-sided waveguide probe antenna and CPW transmission lines matching circuits. The waveguide and device recess features of the metal block are fabricated by a procedure involving multiple stamping and milling steps and resulting to micron-precise feature reproducibility. The devices are fabricated with 3.5-nm NbN films on 2-μm-thick Silicon substrate and beamleads are used for contacts. Several wafers were fabricated having LFA devices of various types.

Fig. 9 shows a scanning electron microscope (SEM) picture of one of such devices. For upGREAT, deposition of the NbN layer was further optimized to thinner layers in order to meet the LO requirements of the array. In comparison to the devices fabricated for the GREAT H channel [23], the LO power requirement was reduced by a factor of 3. HEB microbridge dimensions where reduced from 5.5 × 300 × 3600 to 3.5 nm × 200 nm × 3250 nm with an impedance required by the on-chip circuit of 120 Ω. The typical T_c of the HEBs are 8.1±0.3 K. The horns are electroformed and are spline smooth-walled horns, designed and fabricated by Radiometer Physics GmbH [36].

The average performance of the HEB measured during RF qualification at KOSMA was an uncorrected DSB noise temperature of 800 K±50 K for the 15 mixers qualified for upGREAT and their 3 dB noise bandwidth was 3.7±0.1 GHz (Fig. 10). Compared with the GREAT L2 mixer, the T_{REC} are equal or better and due to the NbN layers, the IF noise bandwidth is much improved (2.3 GHz for NbTiN devices, see Fig. 16). A strong influence of on-wafer position of the devices on LO power requirement was found and is thought to be a result of the inhomogenities of the thinner NbN film. Hence, for each, the subarray devices from one section were selected in order to ensure uniformity of LO power required. The so-called "R" devices were used for the H pol array and "J" devices for the V pol array.

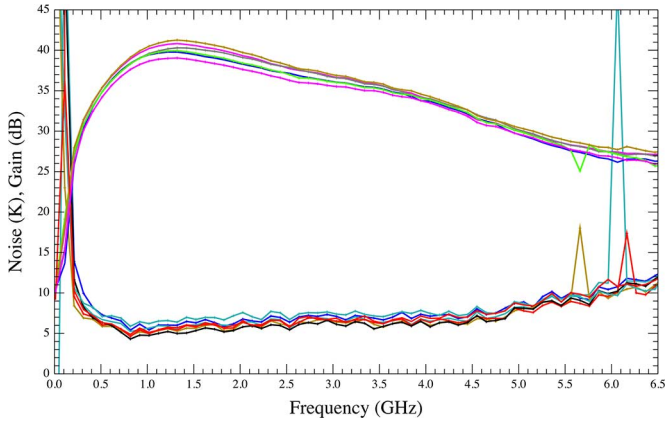

Fig. 11. Measurements for 15 cryogenic LNAs CITLF4 after modification and inclusion of a coil-based bias-T for biasing of the HEB mixers. The gain when measured at 23 K is between 35–40 dB and the noise temperature is 4–5 K between 0.5–4 GHz of IF bandwidth. The resonances above 5 GHz are due to the coil.

The "J" devices require two to three times more LO power than the R devices, which can be attributed to their higher I_C values, 250 μA versus 180 μA, respectively.

2) HFA HEB Mixers: The mixers for the HFA receiver are based on the H-channel HEB mixer [23]. As for the LFA, the HFA devices will use the same wafer with thinner NbN as compared to the H channel mixers. For the HFA array LO power is not as sparse as with the LFA due to the QCL based LO, which provides more output power. Hence, the devices selected should easily meet the requirements and allow efficient beam splitter coupling. The expected noise temperature should be comparable to the measured H-channel mixer results, which achieved 800 K DSB and an IF noise bandwidth of 3.5 GHz, comparable to the LFA mixers. The new mixers were fabricated in parallel with the LFA devices on the same wafers and the selection of the best devices and their characterization will take place end of 2015. Integration in the HFA receiver is scheduled for the first quarter of 2016.

G. IF Signal Processing

The HEB output IF signal in the range 0.5–4 GHz is amplified by a set of SiGe cryogenic LNAs CITLF4 [37], which have nominally a low thermal dissipation of 12 mW. This can be lowered, if required, to 6 mW with little impact on the cryogenic LNA noise temperature performance. Fig. 11 shows 15 cryogenic amplifier characteristics, having a gain of 35–40 dB and a noise temperature of 4–5 K when measured at 23 K physical temperature. These LNAs also include the bias-T for the HEB mixer biasing. The default 5 K resistors provided for that purpose for the CITLF4 models were removed and replaced by custom-made coils. This improved the noise temperature by $\sim$1 K. The cryostat output IF signals are then further amplified by room-temperature LNAs from MITEQ (AFS4), and afterwards processed by room temperature components (amplifiers, filters, equalizers, and variable attenuators) located in in a dedicated IF processor (Fig. 12).

Finally, the signals are fed into an MPIfR-built fast Fourier transform spectrometers with 4 GHz of instantaneous bandwidth (FFTS-4G, Figs. 12 and 13). They are conceptually

Fig. 12. upGREAT IF processor, located in the lower half, contains up to 22 cartridges. Each of them is amplifying, filtering, equalizing, and performing remote control leveling of its IF power to provide the nominal input power to the spectrometers. The upper half of the picture shows the FFTS-4G spectrometers. In this case 16 boards are installed.

Fig. 13. FFTS-4G boards, using the VIRTEX-7 FPGA, two Hittite ADCs with 6-GHz input bandwidth are interleaved. Each board is capable of instantaneously sampling the 0–4 GHz band with up to 64 K spectral channels. For the upGREAT receivers, the number of channels is 32 K.

based on the 0–2.5-GHz FFTS spectrometers [38], [39] and this newer generation is able of instantaneously sampling the 0–4 GHz range using its base band (but can also sample the 4–8 GHz region if using its first Nyquist band).

Each FFT-4G board uses two Hittite 8-bit ADCs (HMC5448) which are time interleaved. The number of channels used for upGREAT is 32 K, obtaining a channel spacing of 122 kHz with an equivalent noise bandwidth (ENBW) of 142 kHz.

IV. LFA Receiver Integration and Laboratory Results

A. Focal Plane Arrays and Cryostat Components

The final integration of all LFA HEB mixers in the cryostat took place in February 2015. A mixer subarray is shown in Fig. 14, with the six offset mixers in place. The inner cryostat assembly can be seen in Fig. 15. A hexagonal grid is chosen for

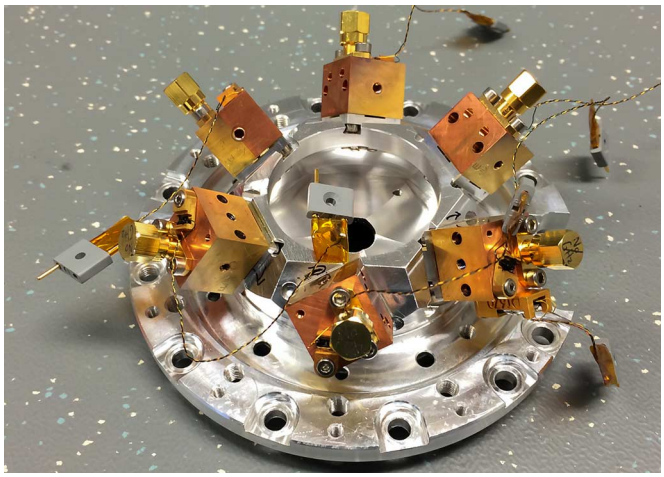

Fig. 14. One of the LFA subarrays HEB mixers mounted on its support structure. The central part accommodates offset parabolic mirrors, placed in a 12-mm side hexagonal configuration, defining the pixel spacing. Only the six offsets pixels are mounted there and the central pixel has a separate mounting structure not shown in the picture.

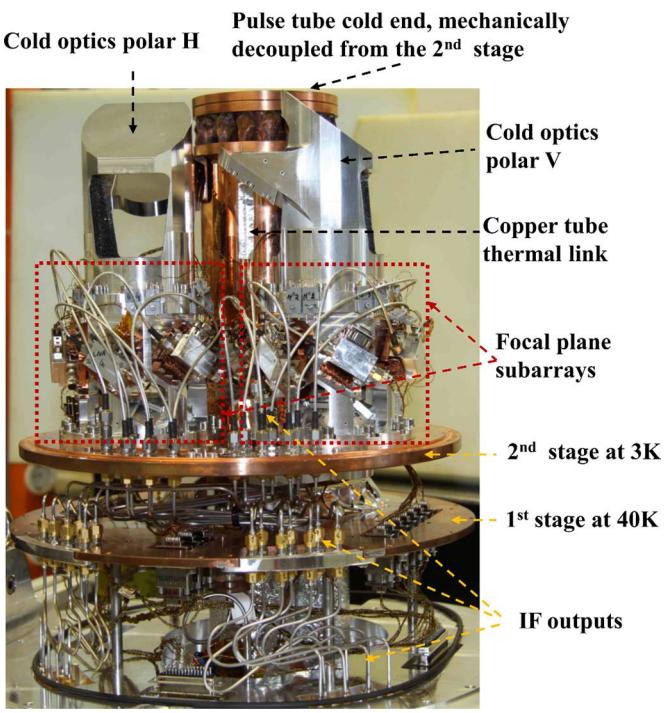

Fig. 15. LFA cryostat 4 K components. The two subarrays can be seen, located symmetrically with respect to the copper heat sink tube, which provides cooling to the 4 K stage plate. The mixers are located inside the aluminum towers and surrounded by the cryogenic low noise amplifiers. The IF outputs are then connected via flexible coaxial lines to feedthrough SMA connectors and then connected via stainless steel coaxial conductors to the cryostat output SMA connectors.

the upGREAT arrays to maximize the packing density and thus the mapping efficiency for compact sources.

The offset mixers are located around aluminum towers providing support for the mirrors and cryogenic LNAs. The IF outputs are then connected via flexible coaxial lines to feedthrough SMA connectors, and then connected via stainless steel coaxial conductors to the cryostat output SMA connectors.

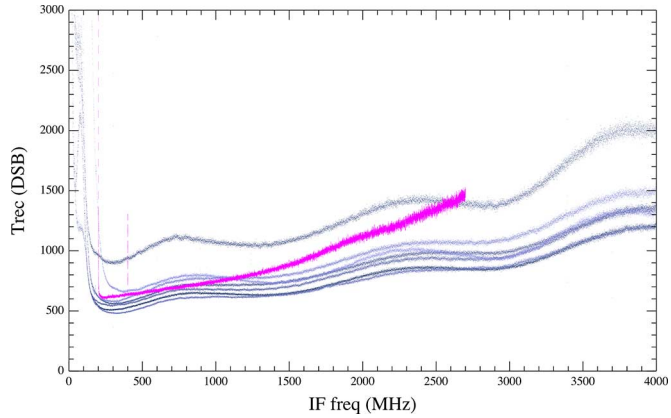

Fig. 16. Uncorrected T_{REC} DSB (K) at 1.9 THz versus IF frequency for the H-polarization LFA 7 channels. The noise IF bandwidth is about 3.3 GHz. The minimum noise temperature (DSB) for the best six pixels is between 500–700 K. One mixer is underpumped and therefore that channel noise temperature degrades to about 1000 K. As a comparison, the performance of the single pixel L2 receiver is shown in purple. Its noise IF bandwidth is smaller (~2.5 GHz) as it uses a NbTiN HEB mixer.

TABLE VII
UPGREAT—LFA SENSITIVITIES

	H-Polarization	V-Polarization
LO Bandwidth	1.88 – 1.92 THz	1.88 – 1.92 THz
T_{REC} (DSB)	~600K at 500 MHz IF [1] ~1200Kat 3500 MHz IF	~1300K at 500 MHz IF [2] ~2600K at 3500 MHz IF
LO coupling	Beamsplitter– 18% coupling	Beamsplitter– 40% coupling

[1-2]Performance for 6 out of 7 pixels, the 7th pixel is underpumped and is about 40% noisier

B. Receiver Characterization

1) LO Coupling: As the LO multiplier chains for the LFA receiver provided sufficient power at the [CII] frequency (1.9005 THz), the preferred coupling optics was using beam-splitter wire grids rather than diplexers. Both optics were tested but the best results were achieved with the beam-splitter coupling scheme. However, strong interferences between the two LO chains when operated in parallel, impeded the simultaneous use of both sub-arrays during the first commissioning.

2) Noise Temperature Measurements: When using the beam-splitter optics plate, the H-polarization subarray which carries the R-section HEB devices needed to have about 18% of the LO power coupled. The other polarization (V) using the J-sector devices needed about 40% LO coupling.

We measured the noise temperature of the whole receiver, evacuating on the optical compartment to simulate the flight conditions at an altitude above 40000 feet. We use an absorber cooled to liquid nitrogen temperature as a cold load and a SiC with Stycast hot load absorber (loads at 77 K and 295 K) [22].

The uncorrected noise temperatures include all of the contributions from the IF chain, HEB mixer, infrared filter, RF window, and signal/coupling losses (shown in Fig. 16 and summarized in Table VII). The noise IF bandwidth is about 3.5 GHz. The minimum noise temperature (DSB) for the best six pixels of the H-polarization array is between 500–700 K. One mixer is underpumped and therefore that channel noise temperature degrades to about 1000 K. As a comparison, the performance

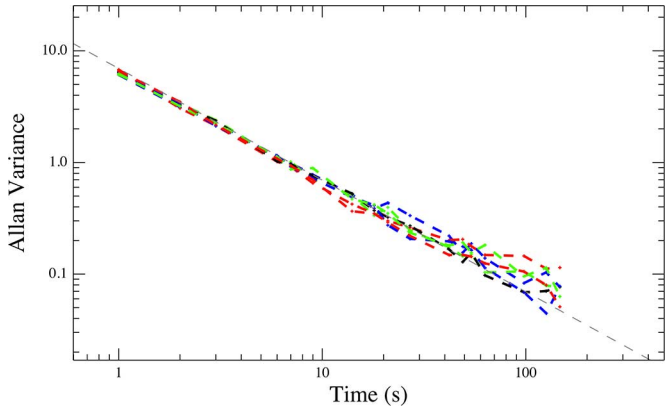

Fig. 17. Example of spectroscopic Allan Variance performed at an LO of 1.902 THz. The compared spectrometer channels have a 1.4-MHz effective bandwidth and are spaced by 700 MHz. Typical Allan times are above 80 s.

of the single pixel GREAT L2 receiver is shown in purple in Fig. 16.

For the V-polarization array, the uncorrected noise temperatures at 1.9 THz are about a factor of 2 worse than the H-polarization, with minimum noise temperatures (DSB) of about 1300 K. This is due to the higher LO coupling required to pump the mixers (40% coupling needed). We are currently replacing the second polarization mixers with devices requiring less LO power which will result in an improved signal coupling.

3) Beam Characterization: Beam characterization and alignment are performed in an iterative fashion. In the MPIfR laboratory in Bonn, optical and radio alignment were made by using a dedicated rotating wheel which allows deriving the average positions for all the pixels in a location close to the telescope focal plane. Then far distance beam measurements at distances ranging from 500 to 2000 mm from the telescope waist position were performed. Beam propagation direction and beam characteristics can then be derived for the individual pixels. By slightly adjusting the cold optics and verifying the applied changes, the beam characteristics were confirmed to be sufficiently close to the designed values.

4) Receiver Stability: Another important figure of merit for the receivers is the total power and spectroscopic stabilities. This will directly impact on the quality of the observations (e.g., unstable bandpass renders line profiles analysis more difficult).

There are numerous potential factors than can impact and limit the receiver stability, for example, pulse tube cooler temperature fluctuations and vibrations, telescope elevation changes, microphonics in the optical compartment, LO cooler temperature fluctuations and vibrations, LO chains output power stability, VDI driver synthesizer output power stability, HEB gain stability, IF components gain variations, and spectrometer stability. A convenient way to assess the overall total power and spectroscopic stability of a receiver is using the Allan variance [40]. We characterized the LFA receiver at various frequencies and bias conditions and the measurements show low total power Allan variance times (3–5 s) in a 1.4-MHz measurement bandwidth. The spectroscopic Allan variance times comparing 1.4-MHz spectrometer channels spaced by 700 MHz are better than 80–100 s (Fig. 17).

The stability is probably slightly worse than the single pixel GREAT receivers which had spectroscopic Allan times above 100 s, after optimization over several observing campaigns. The current performance is already sufficient for efficient observations. By knowing the receiver stability values, the observations modes can be optimized to provide best quality baselines.

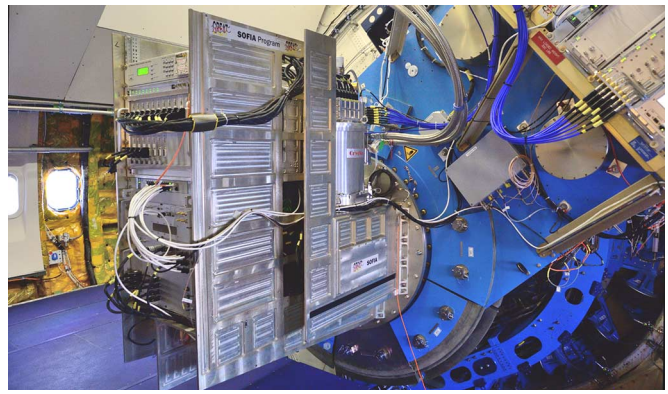

Fig. 18. GREAT/upGREAT instrument mounted on the Nasmyth tube of the SOFIA telescope. On the left side, the electronics rack houses the sensitive bias electronics, reference synthesizers and other motor controllers. The LFA cryostat can be partly seen on the right hand side of the central instrument structure. The pressurized helium hoses can be seen going from the rotary valve on the cryostat to the top part. Fifteen coaxial blue lines (14 for the LFA receiver and 1 for the L1 receiver) connect the cryostats IF outputs to the IF processors and spectrometers FFTS-4G.

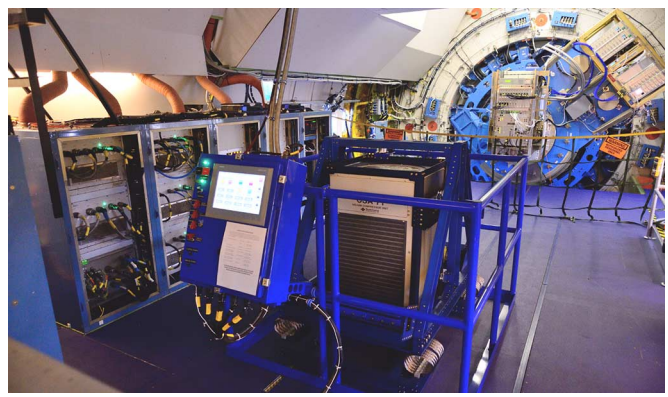

Fig. 19. View from inside the SOFIA aircraft, looking in the aft direction. In the foreground, the Sumitomo CSA-71A compressor can be seen in a vibration-isolated, one-axis Gimbal mount. The electronic control enclosure with a touchscreen panel is mounted to the guard rail. In the background, the GREAT/upGREAT instrument is mounted to the SOFIA telescope's Nasmyth tube flange.

V. Installation and Commissioning Onboard the SOFIA Observatory

A. LFA Receiver Installation

After the successful LFA receiver characterization in the MPIfR facilities, the receiver and all of the associated components and electronics were sent to the NASA Armstrong Flight Research Center (AFRC), Palmdale, CA, USA, in March 2015, where the SOFIA airplane is based. The final characterization was performed in those laboratory facilities using the GREAT mechanical structure, which is the part interfacing with the telescope (Nasmyth tube attachment).

The installation of the upGREAT system aboard the SOFIA observatory took place on May 1, 2015 (Figs. 18 and 19). The

chosen configuration for GREAT/upGREAT was to use in parallel the single pixel L1 receiver (1.25–1.5 THz) together with the LFA receiver. The telescope signal is separated by a QMC low-pass filter dichroic (W1449), letting the 1.25–1.5 THz pass in transmission (95%) and reflecting the frequencies above 1.8 THz (>99%).

After the initial installation onboard SOFIA, the instrument functionalities were verified. Beam measurements close to the telescope focal plane were repeated and an alignment check was performed at the subreflector, using LN_2-cooled absorber material to ensure that the receivers L1-LFA were coaligned and well centered.

For the commissioning flights, both LFA subarrays could not be operated in parallel as the LO chains were causing strong interferences. The H-polarization subarray was therefore selected, having the best performance. The V-polarization subarray was used partially during one flight to verify its on-sky performance and co-alignment with the H-array.

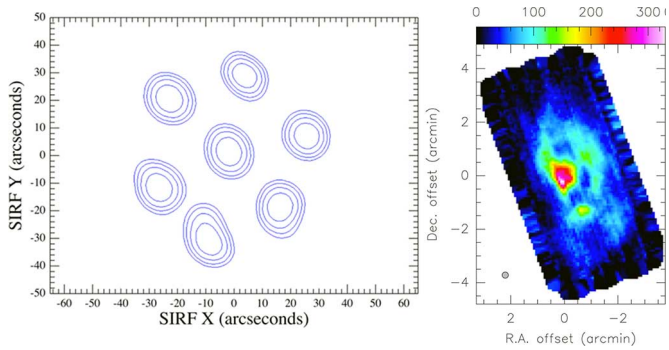

Fig. 20. (a) Preliminary beam maps taken on Saturn, showing the positions of the beams on sky for the H-polarization array. Contours are spaced every 10%. (b) One of the first observations of the S106 nebula using the LFA receiver on May 21, measuring the emission line of ionized atomic carbon [CII] at a wavelength of 158 μm. The effective angular resolution is shown by the circle in the lower left corner.

B. Cryocooler Infrastructure Aboard the SOFIA Airplane

In parallel to the development and testing of the upGREAT instrument in the laboratory facilities, the SOFIA project designed, built, integrated and tested the required associated infrastructure to operate the Pulse Tube cryocoolers aboard the aircraft in 2014–2015, with inputs from MPIfR and cofunded by DLR.

Perhaps the most demanding aspect of this work package was the certification of the various components for airworthiness. Such cryocooler systems are very common on ground-based telescope or hospital magnetic resonance imaging facilities, but are not intended to be operated onboard an airplane. The strong accelerations, turbulence, and tilt angles can cause oil displacement and contamination that compromise the cooling performance of the pulse tube cold head, or might damage the compressor capsule itself in extreme cases. Following recommendations from Sumitomo, it was decided to mount the compressor onto a vibration-isolated, single axis Gimbal mount, to compensate for the airplane accelerations/decelerations in the flight direction and pitch axis tilt. Also, a molecular sieve filter and an additional oil adsorber are mounted externally to the compressor to further reduce the chances of oil contamination reaching the Pulse tube during strong turbulent events.

After developing Concept of Operations and System Specification documents, the NASA Ames group built, assembled and certified the various components comprising this system through a thorough design, testing and validation program. From the pressurized Helium lines, adding up to 35-m length for both return and supply side, to the custom made manifold, which includes various pressure relief valves and burst discs, and the compressor itself, all components and assemblies were certified for compliance with the applicable NASA standards for structural integrity, pressure systems safety, environmental acceptance and airworthiness.

The compressor and control electronics enclosure underwent comprehensive development and environmental acceptance testing (e.g., vibration, temperature, and air pressure). Initial low-amplitude sine sweep vibration testing of the compressor revealed several components and assemblies with natural frequencies that could be excited by aircraft vibrations and lead to potentially damaging resonance, given the damping characteristics of the vibration isolation mounts. These components and assemblies were stiffened to ensure that all natural frequencies were greater than 20 Hz to ruggedize the compressor. The electronic control system incorporates various warning and alarm signals, for the following parameters: roll and pitch angles, vertical and lateral accelerations, various temperatures monitored inside and outside the compressor, and the supply and return pressures of the Helium lines. Exceeding the warning thresholds triggers annunciators to notify the operators, and, if any of the alarm values is reached, the compressor automatically switches off.

C. Commissioning Flights Results

From May 12 to 22, 2015, a series of four commissioning fights was successfully performed. The LFA receiver performed smooth observations during these flights. The receiver sensitivities were as measured in the laboratory, the cryostat second stage temperatures were stable to within 1 mK, independent of the telescope elevation and flight conditions. The commissioning and science observations were of excellent quality, confirming the state of the art sensitivities. Various observing scenarios were performed to validate the in-flight performance of the array. An example of a large-scale on-the-fly mapping of [CII] in S106 is shown in Fig. 20.

The LFA receiver main commissioning results (derived characteristics such as beam efficiencies, beam sizes, observing modes summary, and frequency and intensity calibrations) will be described in [41].

These first series of flight using the LFA receiver also provided substantial data about the associated cryocooler infrastructure. This was essentially a confirmation that the designed system performed nominally. The Gimbal mount allowed operating the compressor during the take-offs, the climbing phase and the entirety of the flights, except for the landing phases, where the compressor was preventively switched off.

VI. Conclusion

We presented the design of the upGREAT THz heterodyne arrays for frequencies of 1.9–2.5 THz (2×7 pixels in orthogonal polarizations) and 4.7 THz (seven pixels in a single polarization). The first array was successful built, tested and commissioned in May 2015 at the [CII] frequency (1.905 THz) with the SOFIA airborne observatory. The performance is state of the art, with $\sim$600 K minimum uncorrected DSB T_{REC}, with a 3-dB noise IF bandwidth of 3.5 GHz for one polarization. The second polarization has $\sim$1300 K minimum uncorrected DSB T_{REC}. We are currently replacing the second polarization mixers with devices requiring less LO power and its performance should then become as good as for the first polarization. Also, a modified LO optical scheme is being implemented, which will allow operating the 14 pixels in parallel. This will be available for the next flight series in December 2015.

A following step will be to employ different local oscillator sources to cover the full 1.9–2.5-THz frequency range. The HFA array receiver at 4.7 THz is currently being integrated and is expected to be commissioned in 2016.

Note Added in Proof

In December 2015, a new flight series with SOFIA has taken place where the second polarization mixers were replaced achieving improved sensitivities (similar to the first polarization mixers) and the optical scheme was modified, allowing us to successfully operate the 14 mixers in parallel.

Acknowledgment

The authors would like to thank S. Türk from the microwave group in MPIfR, Bonn, Germany, for fabricating the stainless steel WR-5 waveguide assemblies used in the local oscillator cooler. They are also very grateful to T. Kerr and G. Petencin from NRAO, Charlottesville, VA, USA, for the copper plating of those waveguides. The authors would also like to thank the strong and constant support of Virginia Diodes Inc. Charlottesville, VA, USA. The KOSMA authors would like to thank M. Schultz for his mechanical design work on the mixer blocks and his perseverance and precision in mounting a large number of HEB devices. Finally, the authors would like to thank the SOFIA Program Office and the staff of the NASA Ames Research Center (ARC) in Moffett Field, CA, USA, and the Armstrong Flight Research Center (AFRC) in Palmdale, CA, USA, for their strong continuous support during the upGREAT commissioning campaign.

References

[1] G. L. Pilbratt *et al.*, "*Herschel Space Observatory*—An ESA facility for far-infrared and submillimetre astronomy," *Astron. Astrophys.*, vol. 518, p. L1, Jul. 2010.

[2] S. W. Holland *et al.*, "SCUBA-2: The 10 000 pixel bolometer camera on the James Clerk Maxwell telescope," *Mon. Not. R. Astron. Soc.*, vol. 430, pp. 2513–2533, Apr. 2013.

[3] G. Siringo *et al.*, "The large APEX Bolometer Camera Laboca," *Astron. Astrophys.*, vol. 497, p. 945, 2009.

[4] C. Ferkinhoff *et al.*, "ZEUS-2: A second generation submillimeter grating spectrometer for exploring distant galaxies," in *Proc. of the SPIE*, 2010, vol. 7741, Art. ID 77410Y.

[5] W. Zhang *et al.*, "Quantum noise in a terahertz hot electron bolometer mixer," *Appl. Phys. Lett.*, vol. 96, 2010, Art. ID 111113.

[6] J. L. Kloosterman *et al.*, "Hot electron bolometer heterodyne receiver with a 4.7-THz quantum cascade laser as a local oscillator," *Appl. Phys. Lett.*, vol. 102, 2013, Art. ID 011123.

[7] C. Groppi and J. Kawamura, "Coherent detector arrays for terahertz astrophysics applications," *IEEE Trans. THz Sci. Technol.*, vol. 1, no. 1, pp. 85–96, Sep. 2011.

[8] U. U. Graf, C. Honingh, K. Jacobs, and J. Stutzki, "Terahertz heterodyne array receivers for astronomy," *J. Infrared Millim. THz Waves*, vol. 36, no. 10, pp. 896–921, 2015.

[9] H. Smith *et al.*, "HARP: A submillimetre heterodyne array receiver operating on the James Clerk Maxwell Telescope," in *Proc. SPIE*, 2008, vol. 7020, no. 70200Z, pp. 1–15.

[10] C. E. Groppi *et al.*, "Testing and integration of supercam, a 64-pixel array receiver for the 350 GHz atmospheric, window," in *Proc. SPIE*, 2010, vol. 7741, pp. 1–11.

[11] U. U. Graf *et al.*, "SMART: The KOSMA sub-millimeter array receiver for two frequencies," in *Proc. 13th Int. Symp. Space THz Technol.*, Cambridge, MA, USA, Mar. 26–28, 2002.

[12] C. Kasemann *et al.*, "CHAMP+: A powerful array receiver for apex," *Proc. of the SPIE*, vol. 6275, Jun. 2006.

[13] C. Walker *et al.*, "The stratospheric THz observatory (STO)," *Proc. SPIE*, vol. 7733, pp. 77330N-1–77330N-9, Jul. 22, 2010.

[14] D. Meledin *et al.*, "A 1.3-THz balanced waveguide HEB mixer for the APEX telescope," *IEEE Trans. Microw. Theory Techn.*, vol. 57, no. 1, pp. 89–98, Jan. 2009.

[15] T. de Graauw *et al.*, "The Herschel-heterodyne instrument for the far-infrared (HIFI)," *Astron. Astrophys*, vol. 518, no. 2, pp. 1–7, 2010.

[16] S. Cherednichenko *et al.*, "2.5 THz multipixel heterodyne receiver based on NbN HEB mixers," *Proc. SPIE*, vol. 6275, pp. 62750I-1–62705I-11, Jun. 2006.

[17] J. Kloosterman *et al.*, "4×1 pixel heterodyne array development at 1.9 THz," in *Proc. 26th Int. Symp. Space THz Technol.*, Cambridge, MA, USA, Mar. 16–18, 2015.

[18] X. X. Liu *et al.*, "A 2×2 array receiver at 1.4 THz based on HEB mixers and a Fourier phase grating local oscillator," in *Proc. 26th Int. Symp. Space Terahertz Technol.*, Cambridge, MA, Mar. 16–18, 2015.

[19] B. D. Jackson *et al.*, "The SPICA-SAFARI detector system: TES detector arrays with frequency division multiplexed SQUID readout," *IEEE Trans. THz Sci. Technol*, vol. 2, no. 1, pp. 12–21, Jan. 2012.

[20] A. Smirnov, "Millimetron: The next step of FIR astronomy," in *Proc. 26th Int. Symp. Space THz Technol.*, Cambridge, MA, USA, Mar. 16–18, 2015.

[21] E. T. Young *et al.*, "Early science with SOFIA, the stratospheric observatory for infrared astronomy," *Astrophys. J. Lett.*, vol. 749, no. 2, Apr. 2012, Art. ID L17.

[22] S. Heyminck, U. U. Graf, R. Güsten, J. Stutzki, H. W. Hübers, and P. Hartogh, "GREAT: The SOFIA high-frequency heterodyne instrument," *Astron. Astrophys.*, vol. 542, no. L1, Jun. 2012.

[23] D. Büchel *et al.*, "4.7 THz superconducting hot electron bolometer waveguide mixer," *IEEE Trans. THz Sci. Technol.*, vol. 5, no. 2, pp. 207–214, Mar. 2015.

[24] R. T. Boreiko and A. L. Betz, "Heterodyne spectroscopy of the 63 μ m OI line in M42," *Astrophys. J.*, vol. 464, pp. L83–L86, 1996.

[25] J. R. Gao *et al.*, "Terahertz heterodyne receiver based on a quantum cascade laser and a superconducting bolometer," *Appl. Phys. Lett.*, vol. 86, 2005, Art. ID 244104.

[26] H.-W. Hübers *et al.*, "Terahertz quantum cascade laser as local oscillator in a heterodyne receiver," *Opt. Exp.*, vol. 13, no. 5890, pp. 5890–5896, 2005.

[27] I. C. Mayorga, A. Schmitz, T. Klein, C. Leinz, and R. Güsten, "First in-field application of a full photonic local oscillator to terahertz astronomy," *IEEE Trans. THz Sci. Technol.*, vol. 2, no. 4, pp. 393–399, Jul. 2012.

[28] T. Crowe, J. Hesler, S. Retzloff, C. Pouzou, and G. Schoenthal, "Solid state LO sources for greater than 2 THz," in *Proc. 22nd Int. Symp. Space THz Technol.*, Tucson, AZ, USA, Apr. 26–28, 2011, Art. ID 11–3.

[29] U. U. Graf and S. Heyminck, "Fourier gratings as submillimeter beam splitters," *IEEE Trans. Antennas Propag.*, vol. 49, no. 4, pp. 542–546, Apr. 2001.

[30] H. Richter, M. Wienold, L. Schrottke, K. Biermann, H. T. Grahn, and H.-W. Hübers, "4.7-THz local oscillator for GREAT," *IEEE Trans. THz Sci. Technol.*, vol. 5, no. 4, pp. 539–545, Jul. 2015.

[31] C. Wang, G. Thummes, and C. Heiden, "A two-stage pulse tube cooler operating below 4 K," *Cryogenics*, vol. 37, pp. 159–167, 1997.

[32] G. Thummes, C. Wang, and C. Heiden, "Small scale 4He liquefaction using a two-stage pulse tube cooler," *Cryogenics*, vol. 38, pp. 337–342, 1998.
[33] A. Wagner-Gentner, U. U. Graf, D. Rabanus, and K. Jacobs, "Low loss THz window," *Infrared Phys. Technol.*, no. 48, pp. 249–253, 2006.
[34] M. Kotiranta, C. Leinz, T. Klein, V. Krozer, and H.-J. Wunsch, "Characterization of imperfections in a martin-pupplett interferometer using ray-tracing," *J. Infrared Millim. THz Waves*, vol. 33, no. 11, pp. 1138–1148, Nov. 2012.
[35] P. Pütz *et al.*, "1.9 THz waveguide HEB mixers for the upGREAT low frequency array," in *Proc. 26th Int. Symp. Space THz Technol.*, Cambridge, MA, USA, Mar. 16–18, 2015.
[36] B. Thomas *et al.*, "1.9–2.5 THz and 4.7 THz electroformed smooth-wall spline feedhorns for the HEB mixers of the upGREAT instrument onboard SOFIA aircraft," in *Proc. 25th Int. Symp. Space THz Technol.*, Moscow, Russia, Apr. 27–30, 2014.
[37] S. Weinreb, "Design of cryogenic SiGe low-noise amplifiers," *IEEE Trans. Microw. Theory Techn.*, vol. 55, no. 11, pp. 2306–2312, Nov. 2007.
[38] B. Klein, S. D. Philipp, R. Güsten, I. Krämer, and D. Samtleben, "A new generation of spectrometers for radio astronomy: Fast Fourier transform spectrometer," in *Proc. SPIE*, 2006, vol. 6275, 2006, Art. ID 62751.
[39] B. Klein, S. Hochgürtel, I. Krämer, A. Bell, and R. Güsten, "High-resolution wide-band fast-Fourier transform spectrometers," *Astron. Astrophys*, vol. 542, p. L3, Jun. 2012.
[40] V. Ossenkopf, "The stability of spectroscopic instruments: A unified Allan variance computation scheme," *Astron. Astrophys.*, vol. 479, pp. 915–926, 2008.
[41] C. Risacher *et al.*, "The upGREAT 1.9 THz multi-pixel high resolution spectrometer for the SOFIA observatory," , unpublished.

Christophe Risacher received the M.Sc. degree from l'École Supérieure d'Électricité (Supélec), Gif-sur-Yvette, France, in 1998, and the Ph.D. degree from Chalmers University of Technology, Göteborg, Sweden, in 2005.

Since 1998, he has worked at various radio astronomy observatories developing novel instrumentation and supporting observations. Among those are the IRAM 30 m telescope in Granada, Spain, the Chalmers University of Technology with the Onsala Observatory, Sweden, the Apex Telescope with the European Southern Observatory, the HIFI instrument with the Herschel Observatory. Since 2011, He is working at the Max Planck Institut für Radioastronomie in Bonn, Germany, and is the project manager responsible for the development of the upGREAT array receivers for the SOFIA NASA/DLR airborne observatory.

Rolf Güsten, photograph and biography not available at the time of publication.

Jürgen Stutzki, photograph and biography not available at the time of publication.

Heinz-Wilhem Hübers, photograph and biography not available at the time of publication.

Denis Büchel received the B.S. and M.S. degree in physics from the Universität zu Köln, Germany, in 2009 and 2012, respectively. He is currently working toward the Ph.D. degree in physics at the Kölner Observatorium für Submm Astronomie (KOSMA), Universität zu Köln, Germany.

His main research interest are development and characterization of superconducting hot electron bolometer mixers for the upGREAT focal plane array extension on SOFIA.

Urs U. Graf, photograph and biography not available at the time of publication.

Stefan Heyminck, photograph and biography not available at the time of publication.

Cornelia E. Honingh, photograph and biography not available at the time of publication.

Karl Jacobs, photograph and biography not available at the time of publication.

Bernd Klein, photograph and biography not available at the time of publication.

Thomas Klein, photograph and biography not available at the time of publication.

Christian Leinz, photograph and biography not available at the time of publication.

Patrick Pütz received the Diploma and Ph.D. degree in physics from the University of Cologne, Köln, Germany, in 1997 and 2003, respectively.

He is a Senior Scientist with the Kölner Observatorium für Submm Astronomie (KOSMA), Universität zu Köln, Germany. He joined the KOSMA instrumentation group for his diploma thesis developing microfabrication processes for submicron area superconductor-insulator-superconductor (SIS) tunnel junction mixers and continued this work for his Ph.D. After graduation, he was part of the Cologne team for the Band 2 SIS mixers for HIFI on Herschel. In 2005 he joined the SORAL instrumentation group at University of Arizona, where he worked on several submillimeter and THz heterodyne receiver projects and related fabrication technology. In 2007 he re-joined KOSMA for work on 1.4 to 2.5 THz waveguide hot electron bolometer (HEB) mixers for the GREAT heterodyne instrument on SOFIA and, in 2011, the 1.9 THz mixers for the Stratospheric THz Observatory (STO). He currently is working on the HEB mixers for the upGREAT focal plane array extension for operating frequencies up to 4.7 THz. His current interests include THz waveguide and planar circuit technology for superconducting devices.

Nicolas Reyes, photograph and biography not available at the time of publication.

Oliver Ricken, photograph and biography not available at the time of publication.

Hans-Joachim Wunsch, photograph and biography not available at the time of publication.

Paul Fusco, photograph and biography not available at the time of publication.

Stefan Rosner, photograph and biography not available at the time of publication.